pVPD Simulations

W.J. Llope, John Mitchell, F. Geurts

March 6, 2000

STAR NOTE 416

Abstract

Simulations specifically on the performance of the pVPD for providing "start signals" to the TOFp system are described. Considerable attention is paid to the definition of the quantity "hits" in the simulations. The results on the pVPD performance for providing fast starts in full energy Au+Au and Si+Si events over a range of impact parameters and pVPD positions will be presented. We find the performance of a 6 channel (3 per side) pVPD is excellent in practically any Au+Au collision in STAR's acceptance. The position of the pVPD that optimizes the performance is just outside the beam pipe and at a $|Z|$ position in STAR in the range of 4.5 to 5 meters, which is a viable location mechanically. The pVPD system also works very well in the Si+Si collisions that were studied ($b \leq 3$fm). All indications are that a six channel pVPD at $Z \sim 4.5$m can meet all performance goals in RHIC heavy-ion running.

1 Introduction

STAR simulations results already exist [1] for the yet unconstructed Vertex Position Detector (VPD), a 48 channel device intended to provide information to the STAR Level-0 trigger on primary vertex location via fast timing. Such a channel count is needed to retain a high efficiency in p+p collisions, where there are very few very-forward tracks. The VPD construction, presently unscheduled, is classified as part of the SVT project and recent results from the bench have been reported by this group [2]. We have been working with the blessings of the SVT and TRG Groups to bring to bear more immediately a version of this detector which we call the Pseudo-VPD (pVPD). The primary job of the pVPD is not the same as that of the VPD. The major goal of the Pseudo-VPD is rather to provide to the TOFp Rack a single high-resolution "start signal" to be used by TOFp systems for track Time-Of-Flight measurements. The pVPD's funding, construction, and commissioning are already handled as part of the TOFp construction project, while its experimental control, digitization, and insertion into the STAR data stream are also via TOFp equipment.

In the first few years of physics running, RHIC is primarily filled with Au nuclei. While the pVPD is expected to be capable of precise primary vertex location in all but p+p and the very lightest nuclear collisions, the desired functionality of the pVPD focusses rather on providing to TOFp fast starts in the heavier collisions happening early on at RHIC. Simulations results on specifically this functionality are not

available as far as we know. In the interest of avoiding what may be unnecessary complications in the primarily Au+Au environment, we are most interested in considering a pVPD with a total channel count *much* lower than the VPD's 48, say six (three per side).[1] However, questions on the start timing performance of such in implementation in the most peripheral Au+Au collisions thus become highly relevant. There is also the possibility of much desired Si+Si running, for which one also wonders if a six channel pVPD can be expected to perform adequately. To address these questions, a six channel pVPD was implemented in GSTAR and its performance specifically for providing fast starts in Si+Si and Au+Au collisions was investigated over ranges of impact parameters in both Venus and Hijing events. Eight different pVPD positions, including four positions in Z and two in R, were studied. The simulations details and results are discussed in this note.

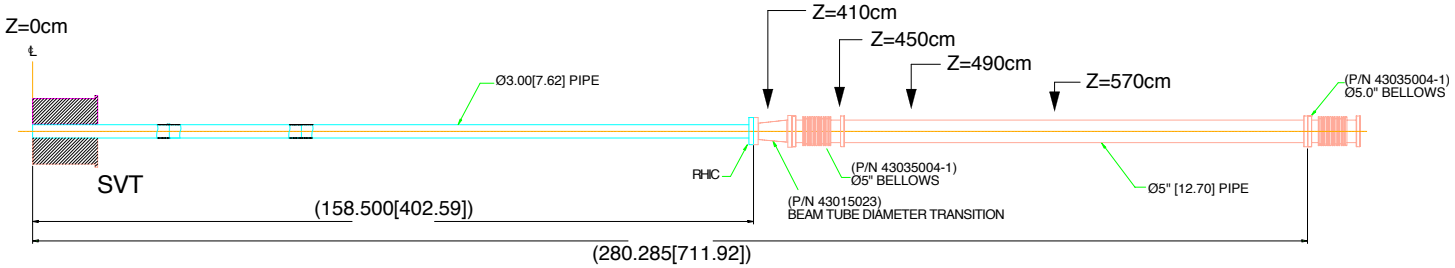

Figure 1: A Side view of the STAR beam pipe from Ref. [3]. The dimensions are labelled in the form inches[cm], while the pipe dimensions labelled are outer diameters.

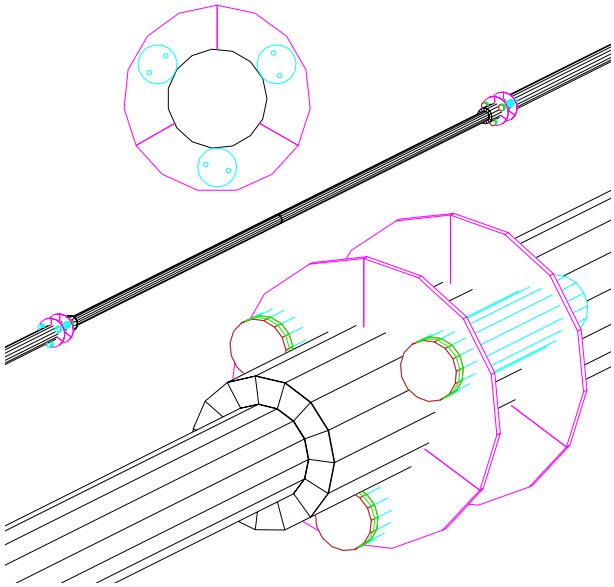

Figure 2: A view along the beam pipe (upper) and two isometric views of the GSTAR implementation of the beam pipe and the pVPD. For this picture the pVPD detectors are positioned at 410cm in Z and an detector inner radius of 6.5cm.

A side view of the STAR beam pipe is shown in Figure 1, while depictions of

[1] The system could of course be expanded in channel count rather easily as an upgrade in preparation for significant p+p or very light ion running.

the pVPD implementation in GSTAR are shown in Figure 2. The mounting structure seen in Figure 2 is the STAR default - there was no attempt made to implement the actual pVPD mounting structure in GSTAR. The pVPD detector system consists of two identical detector assemblies, one on each side of STAR, which are each positioned very close to but not touching the beam pipe and at Z positions in STAR in the range of ∼4-6 meters. Each mounting assembly is mechanically Delrin plastic which mounts to the "Support Beam" [3]. Three PMT assemblies are attached with screws to the Delrin mounting structure. There are thus six channels in the pVPD detector in total. Each PMT assembly consists of a 1/4"-thick layer of Pb and 1/4"-thick layer of Bicron BC-422 plastic scintillator which are glued onto the photocathode of a Hamamatsu R2083 PMT in a "flash-light" design. Each PMT assembly is shielded in a steel tube that is approximately 13" long, *i.e.* somewhat longer than a Pb/Scint/PMT/Base assembly. Scintillator is used in the detector instead of quartz given the higher light output per hit and hence better performance. The simulations assume this in that the quantity used to indicate the "measured" signal in each detector is built from particle energy loss in the active layers, not the number of particles with velocities above a certain threshold (more below).

We intend to use existing (non-mesh) PMTs in the pVPD, which despite the best shield configuration possible, implies that there is a minimum distance from STAR's origin where sufficient shielding is possible. There are also limits on the location of the pVPD detectors along the beam pipe that are imposed by the availability of the space, and the structures, to physically mount to detector. [4] These constraints both imply that the pVPD can sit at positions along the pipe no closer than $Z \gtrsim 4$ meters. Minimum radii for the detector elements are imposed by the radius of the beam pipe at such Z locations. We are not allowed to mount off of or even touch the beam pipe with any part of the pVPD.

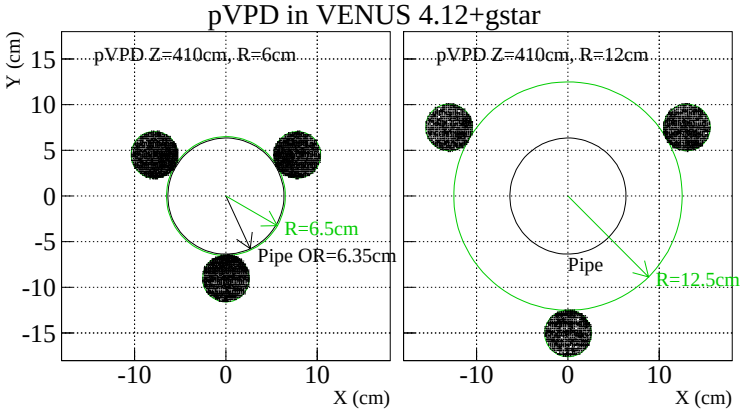

Figure 3: The (X,Y) positions of pVPD hits for the two pVPD detector radii (green) studied here, "R=6 cm" on the left and "R=12 cm" on the right. The beam pipe is shown in black.

We therefore studied the pVPD performance at locations in $|Z|$ of 410cm, 450cm, 490cm, and 570cm. These values are those of the GEANT mother volume. The Z position in STAR of the scintillator layers is 11 cm smaller, i.e. $|Z_{scint}|=|Z|-11$cm. The two halves of the pVPD are always positioned at the same absolute value of Z.

According to Figure 1, the outer radius of the actual pipe is 6.35 cm in this range of Z. At each of the four pVPD Z positions studied, we therefore also studied two different "inner radii" for the pVPD detectors with respect to the beam pipe axis. This is depicted in Figure 3, where scatter plots of the (X,Y) positions of pVPD hits are shown for the two pVPD radii studied here. On the left is shown the hit transverse position patterns for the pVPD radial position referred to here as "R=6 cm," while on the right is the same for the radial position we will refer to as "R=12 cm." According to the figure, the "R=6 cm" simulations correspond to an actuall inner radius for the pVPD detectors of 6.5 cm, which is just larger than the 6.35 cm outer radius of the beam pipe. The cases referred to here as "R=12 cm" have an inner radius of the pVPD detectors of 12.5 cm.

According to Figure 1, a $|Z|$ position of 410 cm in these simulations places pVPD elements near the flanges that transition from a 3" O.D. pipe to a 5" O.D. pipe. A pVPD inner radius of 6.5cm leaves only ~1mm of clearance between the detectors and the beam pipe. Thus, the study here of the pVPD at Z and/or R positions very close to the flanges or the pipe is not meant to imply that these are necessarily viable for the actual detector. Rather, these positions were studied more for academic reasons as extreme points the dependence of the pVPD performance on its position.

2 Implementation

According to previous experiments in which such R2083 PMTs were used for fast timing, [5] the approximate dependence of the start time resolution of individual elements of the pVPD, σ_t, on the number of prompt charged particle hits is

$$\sigma_t = 30\text{ps} \oplus \frac{70\text{ps}}{\sqrt{N_{hits}}}. \tag{1}$$

Thus, the evaluation of the performance of the pVPD for providing start signals simply boils down to the proper evaluation of the number of prompt hits per detector element per event. In any event in which there are 2 or more prompt hits in any one detector channel, the pVPD system will provide starts to TOFp with a resolution of ~58ps or better. This is the required timing performance of the pVPD system. However, one must take care to insure that the definition of the quantity N_{hits} that is extracted from GEANT is consistent with the experimental conditions under which this rule was defined. This definition exists on several levels in these simulations as now described.

When using the "single-step option" in the Advanced Geometry Interface to GSTAR/G2T, the traversal of a single charged particle through a scintillator layer is reported by GEANT as a single entry in the pVPD hits table `g2t_vpdd_hits`. The usual variables are saved for each such hit - `volume_id`, `x[3]`, `dE`, `tof`, `ds`, and `s_track`. Without the single-step option, *i.e.* as in the present STAR library version of `vpddgeo.g`, each scintillator is in software subdivided into smaller subcells, and the hit information for a single particle's traversal *of each subcell* are saved by GSTAR. Such a feature controlling the hits definition is useful for "slow simulations," as it

allows one to simulate at the microscopic level (with software beyond GSTAR/G2T) specific detector response effects. However, such a definition of a "hit" obviously leads to reported numbers of hits which are considerably in excess of the actual number of physical particles that have traversed pVPD scintillators. Inferences on the pVPD performance based on equation (1) and using the numbers of hits so defined would then be completely incorrect.

Therefore, for all of the present simulations, we modified locally the `HITS` definition in `vpddgeo.g` to enable the single-step option. A single charged particle - primary or secondary - can leave at most one hit in any single active element of the pVPD. This reconciles the meanings of GEANT's "volume crossing" and our experimental notions of a particle hit in actual scintillators. Also changed locally in `vpddgeo.g` was the software resolution on the variable `tof`, the total flight time of the particle that left a pVPD hit (more below), from 16 to 18 bits. Other dimensions of invisible (massless) volumes in the pVPD geometry description were also increased to allow the full ranges of pVPD positions of interest.

Further description of the present simulations requires some comments on the signal processing in the TOFp Rack which is intended to produce the actual TOFp master start signals. Like in the TOFp system, each pVPD detector element sends a fast PMT signal to front-end electronics (FEE) very close to the detectors which splits each PMT signal into two and discriminates one of the two. The pVPD FEE boards are TOFp FEE boards without any modification. The analog and logic signals from each of the 6 pVPD elements and the 41 TOFp elements are sent over high-performance coaxial cable to the TOFp Rack. Also brought to the TOFp rack is the STAR pretrigger, which is defined by the TRG Group based on the activity in CTB slats. The earliest pVPD detector to fire a pVPD discriminator in a given crossing starts the definition of the TOFp master start. The TOFp signals arrive $\sim$50ns after the pVPD signals, and are digitized using the TDC start and ADC gates derived from the TOFp master start. The absence of the STAR Pretrigger at $\sim$330 ns after this collision is recognized in the TOFp Rack and used to generate "fast-clears". The absence of a Level-0 token 1.5 μs after this collision will also be recognized in the TOFp Rack and used to generate clears. This leads to the best dead-time performance of the system (compared to using longer cables to require the pVPD and TOFp signals arrive after the pre-trigger). While the desired functionality of the pVPD centers on providing TOFp master starts, the NIM logic in the TOFp rack does not rule out the later addition of logic calculating the primary vertex location using the earliest-firing pVPD elements on each side.

The local analysis code in these simulations thus locates the earliest firing pVPD element on each side, provided the energy deposition for this earliest hit is in excess of one quarter of the energy deposition of a minimum-ionizing particle (MIP). Such a minimum requirement on the deposited energy for a hit to be considered as the "earliest" is the software application of the threshold applied in the Leading Edge discriminators in the FEE. Once the earliest-firing pVPD detectors on each side are located in each event, it is only the number of hits in just these two earliest channels in this event that are relevant. The activity in the other four pVPD channels in the event does not contribute to the start time determination.

The primary observable of interest in these simulations is thus *the number of "prompt" (defined below) hits in the detector element on each side which saw the earliest hit with a pulse height larger than 1/4 of that for one MIP.* Prompt hits are indeed are the only hits that contribute to the leading edge of the signals from individual detector elements, so it is their numbers in the earliest-firing detector channels that reflect most directly the start time performance of the pVPD system.

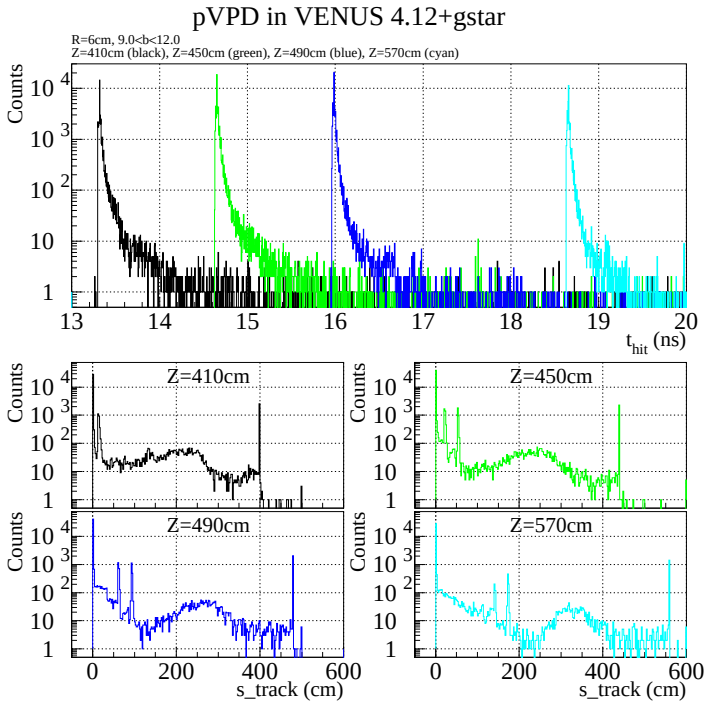

Figure 4: The hit time distributions (upper frame), and the total track length of particles leaving pVPD hits (lower frames) for four different Z positions of the pVPD and Venus Au+Au events with impact parameters in the range of 9 to 12 fm.

In the upper frame of Figure 4, the total flight time distributions from GEANT for particles leaving pVPD hits are shown for four different pVPD Z positions: 410 cm (black), 450 cm (green), 490 cm (blue), and 570 cm (cyan). In all four cases the inner radius, R, is 6 cm, and the events are Venus with impact parameters in the range of 9-12 fm. A hit is defined as "prompt" in these simulations if it within $\pm$25ps of the respective peaks seen in this frame. The ratio of the location of these peaks in time and the respective flight paths are all consistent with particles with a Lorentz $\beta\sim0.9992$ ($\gamma\sim25$). The location of the "prompt hit time cut" is thus simply calculated in a given simulation from the specific value of the pVPD position and β=0.9992. Hits within 25 ps above or below this value are considered prompt. The actual prompt times extracted directly from the simulation and the prompt times from this parameterization for the cut location differ by at most 5ps, which is $1/10^{th}$ of the width of the cut. It therefore appears a valid rule for the present range of pVPD $|Z|$ positions that the earliest pVPD signals from the East(West) detector can be expected to occur at that time after the collision needed for a particle with $\gamma\sim25$ to travel from the primary vertex to the East(West) detector.

The lower frames in Figure 4 are histograms of the total path length of particles leaving hits in the pVPD for each of the same four pVPD Z positions as labelled. Peaks in the lower frames (note the ordinate axis is logarithmic) indicate in each case the three primary sources of hits in a pVPD scintillator. Hits from particles produced in the layer of Pb just in front of this scintillator are seen as the strong peak at `s_track`$\sim$0 in each frame. Hits from primary charged particles are seen as the peak at `s_track`$=Z-11$cm. Hits resulting from particles produced in the pipe and elsewhere in STAR result in the smaller intermediate peaks and broad continua.

It is observed that there is a factor of $\sim$20 more hits in individual pVPD scintillators resulting from particles produced in the Pb layer just in front of this scintillator than resulting from anywhere else. Of the $\sim$5% of the hits coming from "anywhere else," there are about equal amounts of hits resulting from primary charged particles and from charged secondaries produced in the pipe and other structures in STAR.

3 Au+Au Results

The questions motivating these simulations concern the pVPD performance for providing high resolution starts in Au+Au and Si+Si collisions. We have argued that these questions are addressed by properly extracting from a given class of simulated events the number of prompt hits per detector element per event. We have also claimed on the basis of previous implementations of such detectors that if, in any class of events, there exists on average at least one pVPD detector in an event that has seen two or more prompt hits, then the start time resolution of the pVPD system for providing TOFp starts will be quite adequate.

The average numbers of pVPD hits per "earliest detector element" per event in central Au+Au collisions are shown versus the impact parameter in Figure 5. The primary vertex location for all of the present simulations is at Z=0. The two left(right) frames correspond to the East(West) half of the pVPD. The black points depict the average values for all pVPD hits, the average numbers of prompt hits defined as described in the previous section are blue, and the averga enumbers of hits from charged primaries are green. For this figure, the pVPD Z and R parameters used were 410cm and 6cm, respectively.

One notices immediately that there *huge* numbers of prompt hits per detector element per event in the most central Venus Au+Au events. We need not worry at all about the pVPD performance in these events. With up to $\sim$100, and in general many tens, of prompt hits in individual channels of the pVPD, the start time resolution and efficiency will both undoubtedly be excellent. For the remainder of this document then, we will in general no longer discuss Au+Au collisions with b<9fm, as there is no doubt about the success of the pVPD for such events.

However, one also notices that there are on average *ten* hits per pVPD channel in Venus Au+Au collisions at impact parameters near 12 fm. The standard deviation about this mean value is $\sim$4 hits per per detector per event. This implies the pVPD efficiency per event in such such extremely peripheral Au+Au collisions remains well above 90%, and the start time resolution to be expected is $30 \oplus 70/\sqrt{10}$, or $\sim$38

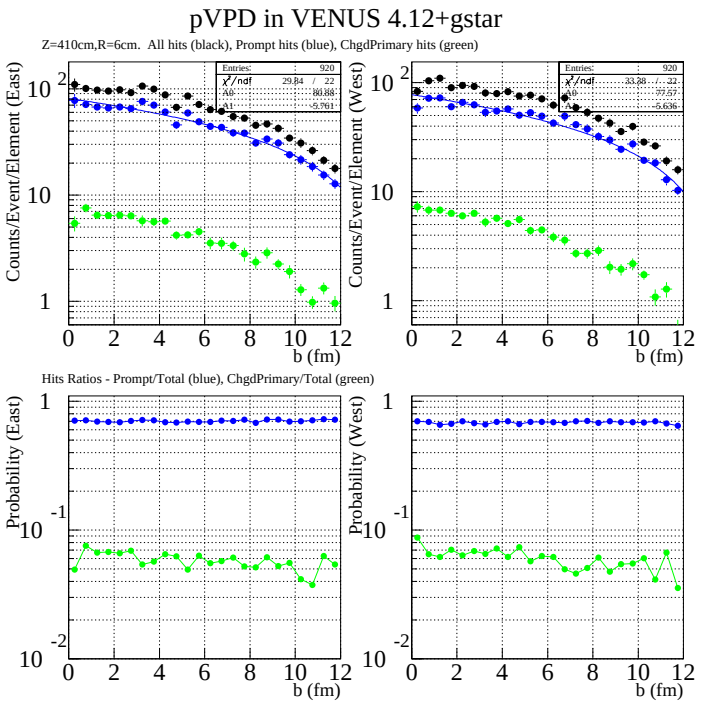

Figure 5: In the upper frames, the number of hits total (black), prompt hits (blue), and charged primary hits (green) for the East (left frames) and West (right frames) pVPD detector per event versus the impact parameter from the full STAR simulation of Venus Au+Au collisions. The pVPD Z and R parameters for this figure were 410cm and 6cm, respectively. The lower frames depict the ratios prompt/total (blue) and charged primary/total (green).

ps. Such resolution is well better than that needed to do good TOFp physics. We therefore expect a pVPD at $|Z|$=410cm to meet all performance goals in Au+Au collisions - even in the most peripheral ones.

The lower frames in Figure 5 depict simply for discussion the ratios of the values shown in the upper frames. The ratio of the number of average numbers of prompt(charged primary) hits per detector channel per event to the average numbers of hits total in the same detectors in the same events are shown as the blue(green) points. In Au+Au collisions and independent of the impact parameter in the range from zero to 12 fm, approximately 70% of the total number of hits in any single detector are prompt, according to the definition described above. This is a reflection of the extremely forward polar angles of the pVPD detectors. Depending on the impact parameter, 4-8% of the hits in any detector element result from charged particles from the primary vertex.

Shown in Figure 6 are the average numbers of total (left), prompt (middle), and charged primary (right) hits per detector per event versus the impact parameter (9fm$<b<$12fm) in Venus Au+Au collisions but for six different combinations of the pVPD positioning parameters Z (410cm, 490cm, and 570cm) and R (6cm and 12cm), as labelled. At any value of the pVPD Z position, increasing the pVPD inner radius from 6.5cm to 12.5cm reduces the number of hits by approximately a factor of two for

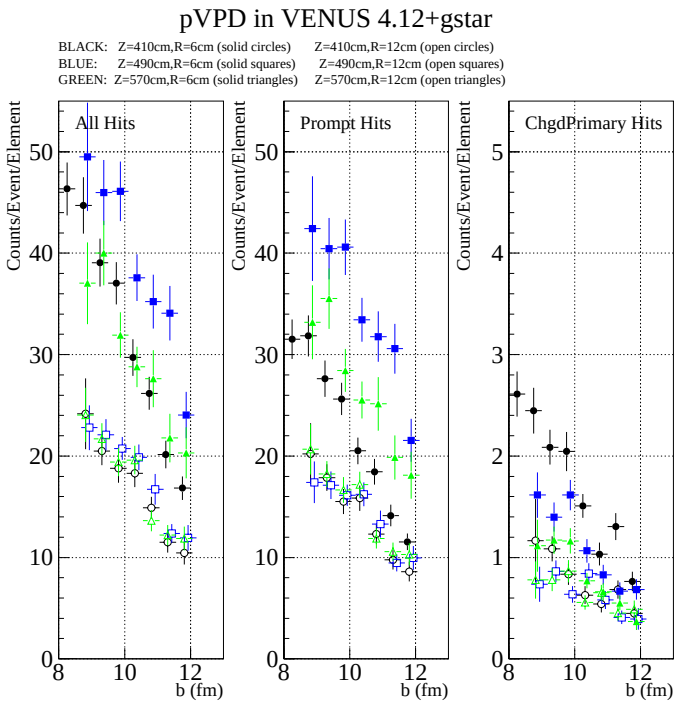

Figure 6: The same as Figure 5 except that the results shown are for 9fm<b<12fm only, and for a number of different pVPD Z and R parameters as labelled.

events with b∼9fm, but only by 30-50% for events with b∼12fm. In none of the cases shown in this figure is the number of prompt hits below ∼8 or so. Hence, the pVPD start timing resolution and efficiency remains excellent in very peripheral Au+Au collisions over wide ranges of the pVPD positioning in both Z and R.

According to Figure 6, the dependence of the number of hits on the pVPD Z position at a given impact parameter is much stronger when the pVPD R=6cm as compared to R=12cm. Plotted in Figure 7 are the average numbers of total (left), prompt (middle), and charged primary (right) hits per detector per event versus the pVPD Z position, at R=6cm and in specific bins of the impact parameter as labelled. In the right frame, the number of hits from charged primaries decreases smoothly with increases in the pVPD Z position at all impact parameters. This is simply the geometrical effect of a decreasing solid angle imposed by single pVPD detectors as they are moved outwards in $|Z|$ away from the primary vertex.

In the middle frame of Figure 7 one indeed sees that there are *maxima* in the dependence of the number of prompt hits per detector channel per event versus the pVPD Z position in all impact parameter bins shown. At b∼6fm there are aproximately 70% more prompt hits per detector element per event when the pVPD is at Z∼5m than there are when the pVPD is positioned near Z±4m or Z±6m. The effect remains as the impact parameter is increased. In Au+Au collisions at b∼11fm one therefore *improves* the start timing resolution of the pVPD (from ∼35.4ps to ∼32.6ps) by moving the pVPD *back* from $|Z|$∼4m to $|Z|$∼5m.

Such a pVPD positioning in $|Z|$ of ∼5m has the additional advantage that the ambient magnetic fringe fields are a factor 3-4 weaker at 5m than they are at 4m.

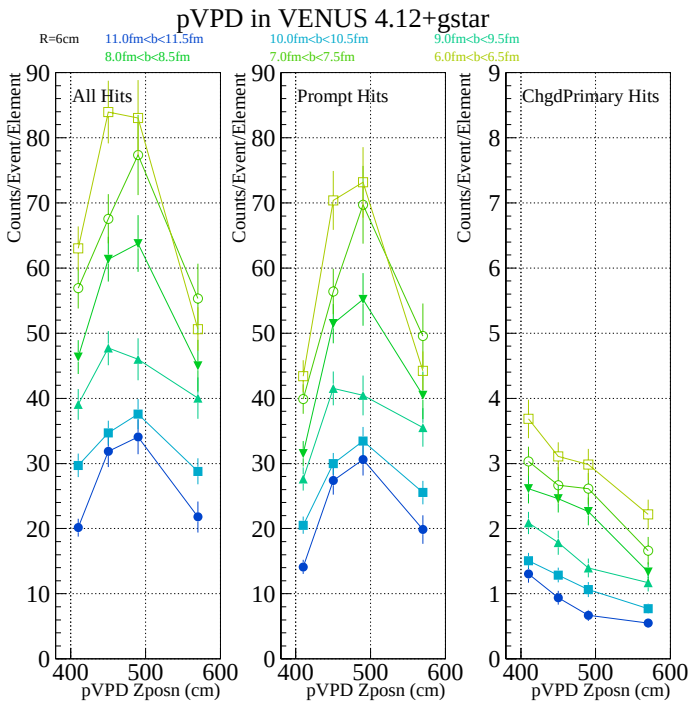

Figure 7: The average numbers of total (left), prompt (middle), and charged primary (right) hits per detector per event versus the pVPD Z position, at R=6cm and in specific bins of the impact parameter as labelled.

According to Ref. [6], the components (B_z, B_r) are approximately (950kG, 100kG) outside the pipe and near Z=4m, and these drop to approximately (280kG, 30kG) at Z=5m. The latter fields can be sufficiently shielded using welded steel tubes with an outer diameter of 2.5" and a length somewhat longer than the actual length of a pVPD Pb/Scint/PMT/base assembly. Thus a pVPD at $|Z|\sim$5m and not 4m allows for somewhat smaller and lighter-weight shields, which reduces the load requirements on the mounting structure. As thinner shields are sufficient, such a pVPD Z position also allows pVPD detectors to sit at somewhat smaller values of R that they could if thicker shields were needed, which also improves the performance slightly.

The maxima in the number of prompt hits versus the pVPD Z position result purely from the specific geometry of the STAR beam pipe. To show this we refer to Figures 8 and 9.

Figure 8 is the same as Figure 7 except that Hijing events were processed in GSTAR, and in only the three most peripheral impact parameter bins. One sees exactly the same trends in Figure 8 that one sees in Figure 7. As might be expected, Venus results in more pVPD hits from charged primaries than does Hijing at the same impact parameter. However, the same very peripheral Hijing events result in more prompt pVPD hits than do Venus events at the same impact parameter. Thus, the pVPD performance and efficiency is superb for RHIC Au+Au events that look like Hijing *and* for RHIC events that look like Venus, even if either is very peripheral.

As maxima are seen in number of hits versus the pVPD Z position in both Venus and Hijing simulations, they are not an artifact of the event generator. Rather, they

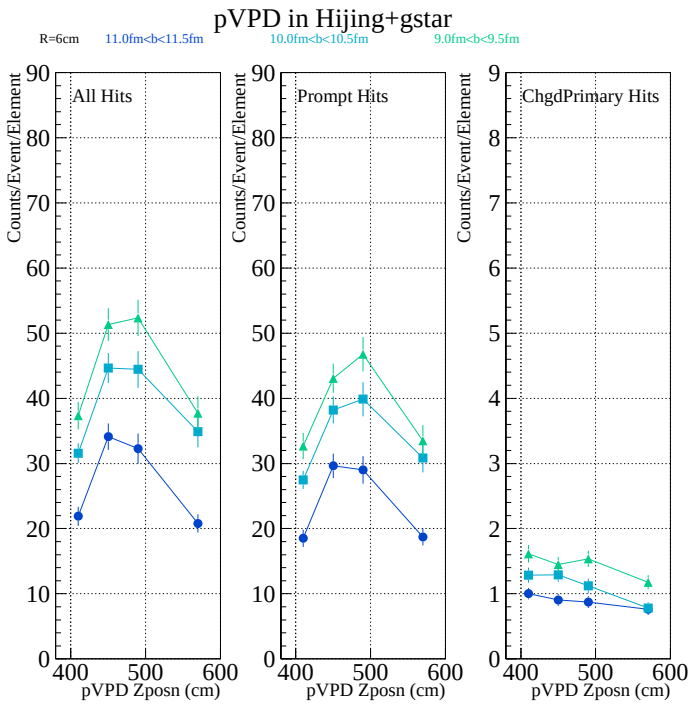

Figure 8: The same as Figure 7 except for Hijing events.

are a result simply of the specific geometry of the beam pipe. A collision at Z=0 occurs at the center of a 3" OD pipe that extends approximately $\pm$4 meters in either direction. At this point in $|Z|$ the 3" OD pipe transitions with flanges and bellows to a 5" OD pipe which extends another 3 meters out to $|Z|\sim$7 meters. If the pVPD is positioned at $|Z|\sim$4 meters, particles leading to pVPD hits have had to travel through only the 3" pipe. Particles resulting in hits in the pVPD when it is positioned near $|Z|\sim$5 meters have had to travel through both the 3" pipe *and* the transition to the 5" pipe.

Shown in Figure 9 are results from simulations that are the same as those for Figure 7 except the pipe geometry was changed into one without the transition to the 5" OD pipe. The 3" OD pipe was extended all the way out to $|Z|$=7 meters. One notices that at Z=410cm in Figures 7 and 9, the number of prompt hits in the modified pipe simulations are, as expected, the same as the numbers of prompt hits from the default pipe simulations. The pVPD cannot "see" the transition when it is at this Z position. However, as the pVPD is moved outward in Z in the various simulations with the modified pipe, the number of prompt hits remains roughly constant, which is not the case in the simulations with the default pipe. This confirms that the transition near $|Z|\sim$4 meters from a 3" to a 5" pipe is the cause of the maxima seen in Figures 7 and 8.

There is also a back-of-the-envelope explanation for these maxima, *cf.* Figure 10. In GSTAR, the transition occurs at $|Z|$=3.806m. The dashed red line is a path from the primary vertex to the "half-way point" in R of the transition from the 3" OD to the 5" OD pipe at Z=3.8m. This path crosses the maximum amount of material in the beam pipe as defined in GSTAR. The polar angle, θ, for this path is ATAN(2"/3.8m), or

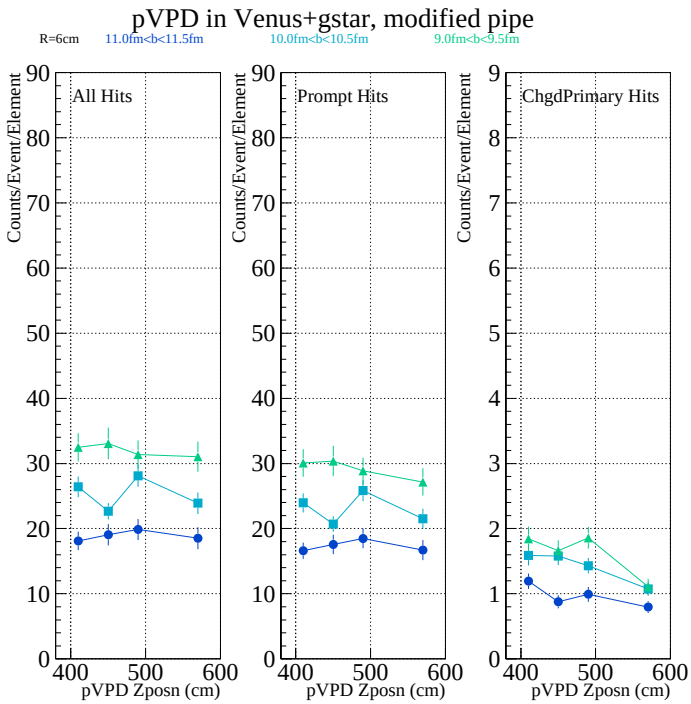

Figure 9: The same as Figure 7 except for a specific modification of the beam pipe geometry.

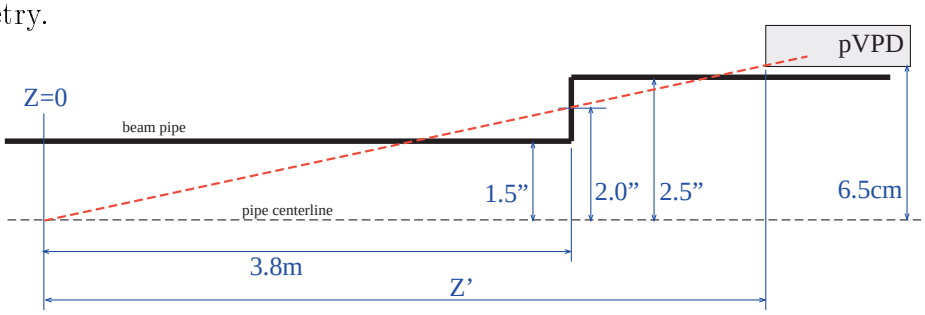

Figure 10: A side view of the pipe (not to scale) indicating the geometrical explanation for the trends seen in Figures 7 and 8.

0.77 degrees. A characteristic location along the pipe, Z', is obtained from this angle and a characteristic radius r for the pVPD via $Z'=r/\text{SIN}(\theta)$, or $Z'\sim 74r$. If one uses for the characteristic radius r=6.5cm, then the characteristic position is Z'=4.8m, which is in agreement with the location of the maxima in Figures 7 and 8.

In a sense, the pipe transition results in an “additional” source of pVPD hits. These can only improve the pVPD performance. If even one hit of this kind occurs within some tens of picoseconds as other prompt hits, the hit contributes to the leading edge of this channel’s signal and hence contributes positively to the start timing performance. As anything occurring in pVPD detectors after the formation of the earliest channel’s leading edge is irrelevant for start timing, hits from such secondaries help if they are prompt and are irrelevant if they aren’t. Further increases in the pVPD $|Z|$ position past 5 meters result in a gradual decrease in the number of hits as solid angle effects take over and the pipe transition becomes a less important

source of hits.

It should be noted that the present simulations do not specifically include the smearing of the primary vertex at the GSTAR-level. The goal here was to investigate specifically the pVPD start time performance over a range of viable pVPD positions and in the general case of collisions near Z=0. A smearing of the primary vertex at the GSTAR-level would only have unnecessarily complicated the analyses for little gain. One can estimate the effects that primary vertices well away from Z=0 have on the pVPD performance from the present results in the following way. The results in Figures 7 and 8 are used as a guide, and we start by assuming that the pVPD is physically positioned at Z=450 cm. A primary vertex at Z=40cm would result in roughly the number of hits in the east(west) detector for the case shown in Figures 7 and 8 where the simulated pVPD sits at Z=410(490) cm. In this manner one estimates that, in an Au+Au collision with a primary vertex location 40cm to one side, there are about the same number of prompt hits in the "near-side" pVPD, and about 30% fewer prompt hits in the "away-side" pVPD. There are on average at least 8 prompt hits in single pVPD channels in even peripheral Au+Au no matter where we put the pVPD in Z in the present simulations (*cf.* Figure 6), which keep the primary vertex at Z=0. The geometry of the pipe is long and uniform, *i.e.* there is just one transition in radius well away at $Z\sim$4m, while a reasonable expectation for the range of primary vertex locations in STAR's acceptance is perhaps $|Z|\lesssim$50cm. The maxima seen in Figures 7 and 8 have a full width in Z of roughly a meter. It is therefore difficult to imagine a pVPD positioned at $|Z|\sim$5m loses much efficiency and resolution for primary vertex location in any, even peripheral, Au+Au collision occurring within $\sim$50cm of Z=0. Put simply, there are always lots of hits available. It should be noted of course that this functionality is secondary in importance to providing good starts to the TOFp Rack. In that vein then, possibly lower numbers of hits in the "away-side" pVPD in a collision at $Z\neq$0 are totally irrelevant, as it is by design the "near-side" pVPD that fires the TOFp master start. Even so, the logic to calculate electronically the locations of primary vertices from the pVPD timing signals is not difficult to implement. This could, once available and if desired, be provided electronically to the STAR TRG for inclusion into Level-0 decision-making. One example of a electronic approach for obtaining this information, and recent bench results, are available from Ref. [2].

4 Si+Si Results

When considering a six-channel pVPD, the initial concerns clearly centered on the affects that the low track count in peripheral Au+Au collisions could have on the pVPD performance. There are mechanical and magnetic field constraints which force out to larger values the detector's position in Z in STAR, which would also be expected to limit the performance of the system. However, the results of the previous section indicate clearly that neither is a significant concern. We find that the pVPD will operate at high efficiency and at a start resolution near $\sim$40ps for practically any Au+Au collision in STAR's acceptance over a wide range of possible positions

for the pVPD. We thus turn now to a discussion of the pVPD performance in Si+Si collisions, for which one's concern about the pVPD performance in very low track multiplicity events must be amplified.

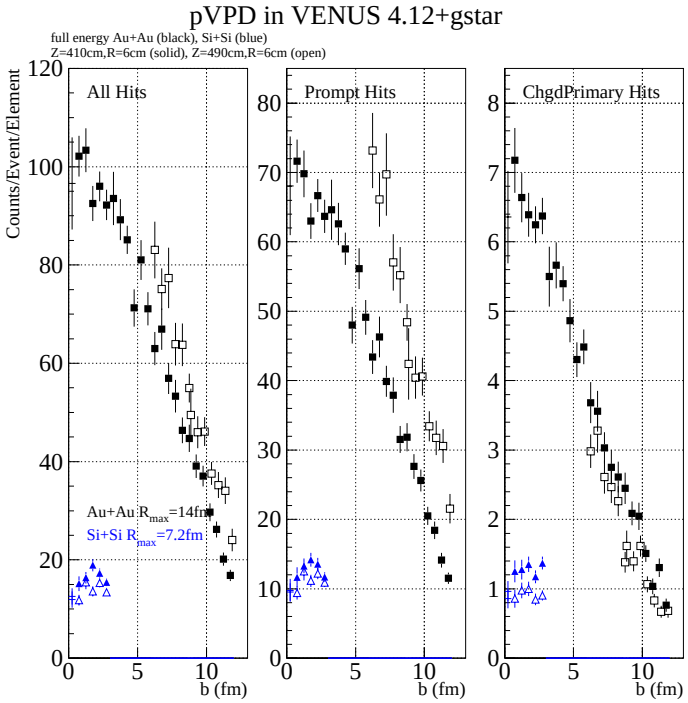

Figure 11: The comparison of the numbers of pVPD hits in Si+Si and Au+Au collisions versus the impact parameter and at two different Z positions of the pVPD, as labelled.

The results for the available Si+Si collisions are shown in Figure 11. The events are Venus in a range of Si+Si impact parameters from 0 to 3 fm. The Si+Si(Au+Au) results at two different pVPD Z positions are shown in blue(black). As there is on average 10 prompt hits per pVPD element per event in Si+Si collisions with $b \lesssim 3$fm, one expects that the pVPD will perform very well for such events. Si+Si events at larger impact parameters are not available in the STAR library. However it is clear from the Figure that the pVPD will still perform adequately for Si+Si impact parameters larger than 3fm, perhaps up to much as $\sim$5fm. This is because an acceptable start time performance is achieved for any event with at least 2 prompt hits, whereas there are still on average $\sim$10 prompt hits in Si+Si collisions at b=3fm.

5 Conclusions

In this note we have described simulations specifically on the start timing performance of a six-channel PMT-based detector called the Pseudo-VPD. Considerable attention was paid to the proper definition and interpretation of the concept of "hits," and to the implementation of logic in the simulations software that is consistent with the pVPD signal processing to be implemented in the TOFp Rack.

In the full GSTAR simulations of both Venus and Hijing collisions of full energy Au nuclei, we observe that a six-channel pVPD should be expected to have a start time resolution on the order of 40ps and an efficiency of practically unity. This good performance results directly from the large numbers of prompt particle hits per pVPD detector channel that are seen in even in the most peripheral collisions. We have also observed that there is a "sweet-spot" for the pVPD positioning in Z resulting from specific details of STAR's geometry, in particular that of the beam pipe and the magnetic fringe fields. A pVPD positioned in $|Z|$ near 5 meters instead of 4 meters sees high rates of prompt hits, magnetic fields small enough to shield easily, and imposes lesser requirements on the pVPD mounting structure. Simulations of Si+Si events predict excellent start timing performance for impact parameters near and below 3fm. While we did not simulate Si+Si collisions at b>3fm, we estimate via extrapolation that the pVPD can still function with some efficiency and resolution in Si+Si impact parameters as large as perhaps 5fm.

Thus, whenever RHIC is filled with heavy-ions, the pVPD is quite sufficient for providing quality start time information to the TOFp system. In a year or so, as the prospect for significant p+p or very light ion running is becoming more real, the pVPD could be upgraded simply by adding a few more detector channels to each side to increase the overall efficiency.

References

[1] Z. Milosevich, http://www.star.bnl.gov/STAR/html/trg_l/VPD/Simulations/-vpd.html (1995);
D. Russ and M. Kaplan, private communication (1999).

[2] wsu description document
sanjeev web page

[3] See STAR Drawing CNV925-E-1, Part number 1, and STAR Drawing CNV926-C-1.

[4] R. Brown, private communication.

[5] Such PMTs were used successfully in the TOF System in the E878, and as start detectors in E866 and E896.

[6] http://duvall.star.bnl.gov/lxr/source/pams/geometry/mfldgeo/mflddat.g